



# The Effect of Carbon Dioxide on the Cycle Life and Electrolyte Stability of Li-Ion Full Cells Containing Silicon Alloy

L. J. Krause,\*<sup>z</sup> V. L. Chevrier,\* L. D. Jensen, and T. Brandt

Corporate Research Materials Laboratory, 3M Center, St. Paul, Minnesota 55144-1000, USA

Carbon dioxide is shown to be an effective additive to standard Li-ion electrolyte for extending the cycle life of full pouch cells containing an engineered silicon alloy. CO<sub>2</sub> was introduced to pouch cells by adding a few milligrams of dry ice to cells before sealing. The cells contained composite negative electrodes formulated with 15 to 17 wt% of an engineered silicon alloy and a LiCoO<sub>2</sub> positive electrode. Parasitic electrolyte reactions were measured in-situ by isothermal micro-calorimetry and high precision coulometry and compared to cells containing 1-fluoro ethylene carbonate (FEC). Extended cycling of cells containing CO<sub>2</sub> were compared to cells containing FEC. Cell gas generation and gas consumption were measured by applying the Archimedes principle. A new approach using small tubes in pouch cells to differentiate volume changes from gassing and solid expansion is introduced. Cells with CO<sub>2</sub> showed significantly lower parasitic thermal power, improved coulombic efficiency and better capacity retention compared to cells containing electrolytes with FEC. The gas generation/consumption experiments showed that Si alloy reacts with CO<sub>2</sub> during cycling until it is fully consumed. Combining FEC and CO<sub>2</sub> reduces the consumption rate of CO<sub>2</sub>. Microscopy of cross-sectioned cycled electrodes showed a thin SEI layer and minimal silicon alloy erosion. The combined work establishes CO<sub>2</sub> as a powerful precursor to an effective SEI layer on silicon alloys. Finally, CO<sub>2</sub> is shown to be an effective SEI former for graphite in EC-free electrolytes.

© The Author(s) 2017. Published by ECS. This is an open access article distributed under the terms of the Creative Commons Attribution 4.0 License (CC BY, <http://creativecommons.org/licenses/by/4.0/>), which permits unrestricted reuse of the work in any medium, provided the original work is properly cited. [DOI: 10.1149/2.1121712jes] All rights reserved.



Manuscript submitted July 17, 2017; revised manuscript received August 8, 2017. Published August 25, 2017.

The desire to increase energy density in Li-ion cells has fueled the research and development of silicon and silicon-based materials as a component of Li-ion negative electrodes. In most cases, however, only small amounts of silicon or silicon alloy are used largely because of the generally inferior cycle life of silicon compared to graphite. While there can be several reasons for the inferior cycle life of silicon and silicon alloys one important contributor to poor cycle life is the erosion of the silicon particle by parasitic electrolyte reactions.<sup>1-3</sup> Because of the volume changes Si experiences during cycling, continuous passivation is required at the surface and the demands on the electrolyte system are greater than for graphite.

Carbon dioxide (CO<sub>2</sub>) has been described as an effective electrolyte additive in metallic Li cells many years ago.<sup>4</sup> In that work it was shown that cycling efficiencies of the Li electrode were greatly increased in the presence of CO<sub>2</sub>. With the development of Li-ion cell chemistry the use of CO<sub>2</sub> was also explored early on.<sup>5-7</sup> In a few papers on the subject it was shown that the CO<sub>2</sub> generators, known as pyrocarbonates, were effective in forming SEI layers on graphite.<sup>8,9</sup> More recently a patent by workers at Sanyo has described the effect of electrolytes containing CO<sub>2</sub> on the cycle life of sintered negative electrodes containing silicon.<sup>10</sup>

In the course of our work on the erosion of silicon alloys our interest was drawn to the role of gas generation in cells of this type. It became apparent that CO<sub>2</sub> was remarkably effective as a precursor to an especially effective SEI layer on silicon alloys, significantly extending the cycle life. The effectiveness of CO<sub>2</sub> was also found to occur on graphite also but the effect is far less dramatic.

## Experimental

**Electrochemical cell construction.**—Machine wound pouch cells were used in this work. They were obtained from LiFUN Technology (Xinma Industry Zone, Hunan Province, China) as sealed dry cells. Two families of cells were tested in the context of this paper. Table I lists the attributes and formulations of the electrodes and cells. The cells that contain silicon alloy, LF129 and LF794, differ in the type of graphite used in the composite negative electrode and the composition and material mix of the conductive diluent. These differences may affect the mechanical failure mechanism from large volume changes of the Si alloy particles though the more significant difference is the

higher areal reversible capacity of LF794 at 3.3 mAh/cm<sup>2</sup> versus 2.6 mAh/cm<sup>2</sup> for LF129 cycled from 3.0 V to 4.25 V. The Si alloy used has a reversible capacity of 1180 mAh/g, a density of 3.5 g/cm<sup>3</sup>, a surface area of 6.9 m<sup>2</sup>/g and a median particle size of 5.2 μm. In cells not using CO<sub>2</sub> the cells were first opened in a dry room and dried at 70°C under vacuum overnight. The cells were then filled with 0.9 g of electrolyte in a dry room with an operating dew point of -50°C. The cell filling procedure employed brief, periodic vacuum degassing in order to allow the electrolyte to access all void volume within the cell's electrodes. The weight before and after the electrolyte filling procedure was recorded in order to ensure the weight of electrolyte added to each cell was consistent. The pouch cells were then sealed under vacuum in a MSK-115A vacuum sealing machine (MTI Corp.) The cells were allowed to stand for 24 hours prior to cycling to ensure complete wetting. In general no charge was applied during standing, in some cases, as noted, a 2 V hold was applied.

**Electrolyte preparation.**—The base electrolyte used in this work was 1 M LiPF<sub>6</sub> in a 3/7 (w/w) blend of ethylene carbonate (EC) and ethyl methyl carbonate (EMC) obtained from BASF and used as received. Vinylene carbonate (VC) was obtained from Novolyte and 1-fluoro ethylene carbonate (FEC) was obtained from BASF and used as received. All solvents, salts and blends were stored in a dry box located within a dry room.

The introduction of CO<sub>2</sub> into the cells was done by two methods. The first involved adding 3 to 7 mg of dry ice in a dry room to the cell previously filled with the base electrolyte and then immediately sealing the cell without degassing. These cells, as they warmed, inflated due to the increased CO<sub>2</sub> gas pressure. To insure that significant excess water was not introduced into the cell by this method we conducted the following test: a sample of base electrolyte was cooled to 5°C by adding solid particles of dry ice in the dry room. The electrolyte was then allowed to warm to room temperature and the water content was then determined by the Karl-Fisher technique. The water concentration in the base electrolyte was found to be between 15 and 30 ppm typically and after the addition of dry ice the water level never exceeded 50 ppm. The second method of introducing CO<sub>2</sub> was to bubble the gas through the electrolyte for approximately 1 hour in order to saturate the electrolyte.<sup>10</sup> A dry cell was then filled with 0.9 g of the saturated electrolyte and sealed without degassing. We note that in both methods eventually the partial pressure of CO<sub>2</sub> rises to a level that results in the pouch cells "pillowing". While this renders this approach commercially impractical for pouch cells, the pouch cells

\*Electrochemical Society Member.

<sup>z</sup>E-mail: [ljkrause@mmm.com](mailto:ljkrause@mmm.com)

**Table I. Specifications the of Li-ion pouch cells used in this study.**

	LF129		LF794		LF44		LF45	
	Negative	Positive	Negative	Positive	Negative	Positive	Negative	Positive
Formulation (w/w)	BTR918/SiAlloy/ KS6/SP/LiPAA*	LiCoO <sub>2</sub>	MAGE/SiAlloy/ KS6/LiPAA	LiCoO <sub>2</sub>	Artificial graphite	LiCoO <sub>2</sub>	Artificial graphite	LiCoO <sub>2</sub>
	70.7/15/4/0.3/10	97	63/17/10/10	97	96	97	96	97
Coating weight (mg/cm <sup>2</sup> )	8.5	20.8	9.2	23.5	9.8	17.7	10	14.1
Nominal Porosity (%)	30	20	30	20	30	20	30	20
Current collector	15 um Cu	20 um Al	15 um Cu	20 um Al	10 um Cu	12 um Al	10 um Cu	12 um Al
Reversible capacity	2.6 mAh/cm <sup>2</sup> (3.0 V–4.25 V)		3.3 mAh/cm <sup>2</sup> (3.0 V – 4.25 V)		2.6 mAh/cm <sup>2</sup> (3.0 V - 4.3 V)		2.8 mAh/cm <sup>2</sup> (3.0 V–4.4 V)	
Balance cutoff voltage	4.35 V		4.35 V		4.4 V		4.5V	
Nominal capacity	220 mAh		290 mAh		250 mAh		240 mAh	

\*LiPAA-based binder.

are convenient for containing the CO<sub>2</sub> and the volume changes allow for straightforward characterization of consumption through volume changes.

**Archimedes measurements of pouch cell volume.**—Pouch cell volumes were measured using the Archimedes method.<sup>11</sup> Pouch cells were suspended from Mettler Toledo balances into beakers of pump oil. Weight measurements were logged using custom software from the balances and volumes calculated using the oil density. Pouch cells were wired using fine magnet wire to minimize the effect of the wires on the weight measurement. Balances and beakers were in a temperature controlled room held at 22°C and protected by a shroud to minimize the impact of air currents.

Volume measurements were also performed with pouch cells containing small open-ended polypropylene tubes. A 2 cm long, 3 mm ID tube was placed inside the pouch cell next to the jelly roll in the pouch area typically reserved for degassing (Figure 5). During degassing the inner volume of the tube is evacuated along with the rest of the cell. The tube provides a ~0.14 mL volume that can then be filled by gas during cell gassing. Since the dimensions of the tube are fixed, the volume increase of the pouch cell will be nearly zero during gassing until the tube is filled with gas up to atmospheric pressure. While gassing will not cause appreciable volume changes, changes in the dimensions of electrodes will still result in measurable volume changes. By comparing the volume changes of a pouch cell with a tube to one without a tube one can quantify the volume changes attributable to solids and to gases. To our knowledge, this approach has not been previously reported in the scientific literature.

**Isothermal heat flow calorimetry.**—Isothermal heat flow calorimetry was conducted using a TAM III (Thermally Activated Module, TA Instruments) in which 12 calorimeters were inserted. The temperature used throughout this work was 37°C. The TAM III is capable of controlling the bath temperature to within a few micro-degrees centigrade. Reference 12 describes the method and modifications made to the TAM III to allow in-operando calorimetry measurements on Li-ion cells. Further details for adapting the TAM III calorimeter to parasitic measurements with pouch cells can be found in Reference 13.

**Electrochemical measurements.**—Electrochemical cycling in the context of thermal measurements was performed with Keithley 2602A source-measure units. This equipment is capable of supplying currents in the 20 mA range with an accuracy of ±0.03% + 6 μA with a resolution of 200 nA. The voltage measurement accuracy is ±0.015% + 1 mV with 10 μV resolution in the 6 V range. Time resolution is <1 sec. This precision allows the measurement of the coulombic efficiency to within ±0.02%.

Electrochemical cycling in the context of Archimedes measurements was performed with a Maccor Series 4000 cyclers. Cycle life

testing was performed with a Neware BTS3000 cycler having a maximal current of 500 mA. High precision cycling was performed with an ultra high precision Novonix cycler.

The protocol for cycling cells in the isothermal heat flow calorimeter was as follows: cells were cycled 10 times in each of the voltage segments of 3.0–3.8, 3.5–3.8, 3.7–3.9, 3.8–4.0, 3.9–4.1 and 4.0–4.25 V. The current for all cycles was 20 mA, nominally C/11 for a full voltage range of 3.0–4.25 V. Ten cycles per voltage segment resulted in a nominally stable coulombic efficiency and average parasitic thermal power for a given voltage segment as described in an earlier publication.<sup>13</sup> The last cycle of each voltage segment was then used to construct a plot of parasitic thermal power versus the average voltage of the segment. We note that in the method we use here, coulombic efficiency, or inefficiency, is simultaneously collected with the thermal data for each voltage segment.

We have reported on this cycling protocol previously in a study of electrolyte chemistry of graphite//LiCoO<sub>2</sub> cells. In the present work, where two materials with distinctly different voltage versus capacity characteristics are considered (i.e. Si and graphite), the lithiation and delithiation does not occur uniformly for both materials under all voltage segments. This was discussed in a previous publication.<sup>3</sup>

**Microcalorimetry data analysis method.**—The treatment of microcalorimetry data to arrive at a parasitic thermal power has been described in detail earlier.<sup>12,13</sup> Here we briefly describe the methods used in the present work. This method, termed the “integration/subtraction” method, yields an average parasitic thermal power at a given average voltage. A total thermal energy is first obtained from the calorimetry data over one cycle. Secondly, the energy loss over one cycle is calculated using the voltage and current (corresponds to the hysteresis area in a voltage-capacity plot). Subtracting the energy loss from the total thermal energy yields a parasitic energy. Dividing the parasitic energy by the cycle time yields an average parasitic thermal power, which can be compared across cycles of various durations.

**Cross sectional microscopy.**—In a dry room, cycled electrodes were rinsed in DMC and ion beam polished cross section were obtained with a JEOL IB-09010CP cross section polisher. Cross section imaging was performed with a Hitachi s-4700 field emission scanning electron microscope (FESEM). More details can be found in Reference 3.

## Results

**Microcalorimetry and imaging.**—Figure 1a shows the capacity versus cycle number of a LF129 cell injected with CO<sub>2</sub> by the dry ice method, a cell containing 10 wt% FEC as an additive to the base electrolyte and a cell cycling only in the base electrolyte (EC/EMC 3/7 1M LiPF<sub>6</sub>). Figure 1b shows the capacity retention normalized at cycle 2 for all three cells. Figures 1a and 1b show a quite flat capacity retention for the cell containing CO<sub>2</sub> with virtually no capacity loss

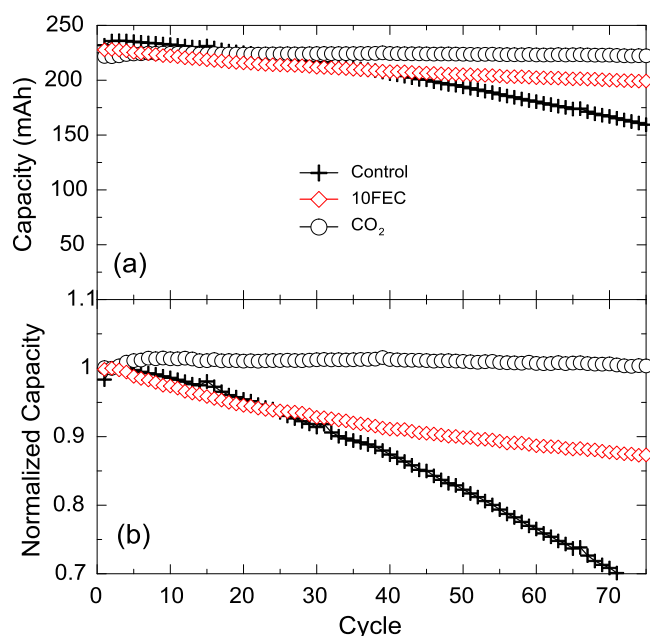


**Figure 1.** Cycling performance of LF129 cells with base electrolyte (EC/EMC 3/7 1M LiPF<sub>6</sub>) and with additives: 10 wt% FEC or CO<sub>2</sub> (dry ice), as indicated. (a) Absolute discharge capacities, (b) discharge capacities normalized to cycle 2.

over 70 cycles at a C/11 rate between a charge voltage of 4.25V and a discharge voltage of 3.0 V. Conversely the cell containing 10 wt% FEC shows a 13% capacity loss under the same cycling conditions and the cell cycling in the base electrolyte shows a nearly 35% capacity loss.

In a previous publication we described the parasitic electrolyte reactions measured by isothermal micro-calorimetry and high precision coulometry of this type of cell cycling in the base electrolyte and with 10 wt% FEC.<sup>3</sup> Figures 2a and 2b show the parasitic thermal power and coulombic inefficiency (CIE = 1-CE) of a cell containing CO<sub>2</sub> charged by the dry ice method and a cell with 10 wt% FEC in the

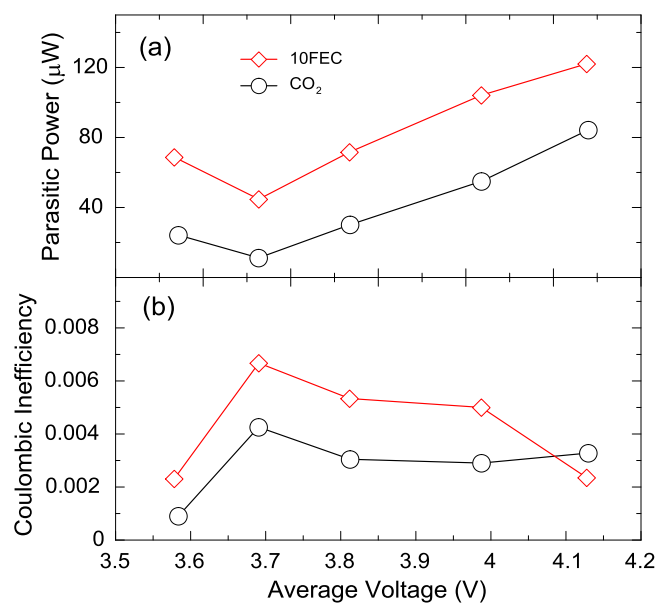


**Figure 2.** (a) Parasitic power and (b) coulombic inefficiency obtained from narrow voltage cycling of LF129 cells with 10 wt% FEC or CO<sub>2</sub> (dry ice) additives added to base electrolyte (EC/EMC 3/7 1M LiPF<sub>6</sub>), as indicated.

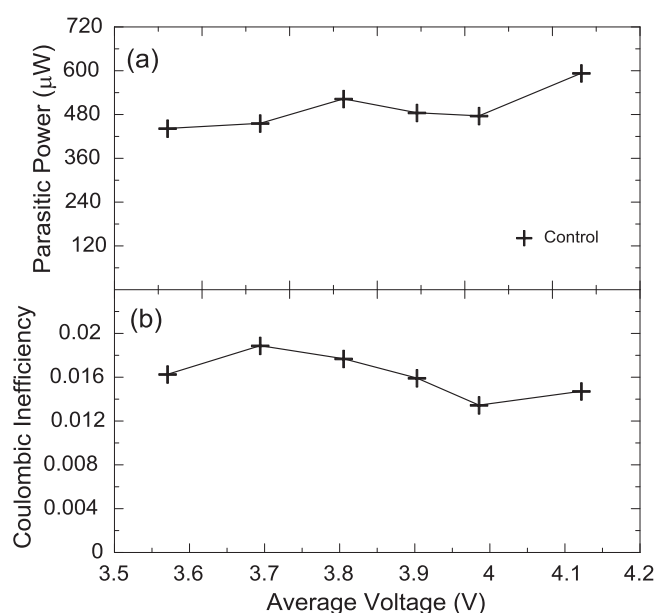


**Figure 3.** (a) Parasitic power and (b) coulombic inefficiency obtained from narrow voltage cycling of LF129 cells with base electrolyte (EC/EMC 3/7 1M LiPF<sub>6</sub>). Note the difference in scale compared to Figure 2.

base electrolyte. These cells were cycled 50x and 42x respectively before they were inserted into the calorimeter. The cell containing CO<sub>2</sub> showed significantly lower parasitic thermal power and the CIE is correlated with the thermal power. This indicates the improved capacity retention shown in Figure 1 is the result of lower parasitic electrolyte reactivity. For comparison purposes, Figure 3 shows a cell with only the base electrolyte which was cycled 45x before insertion into the calorimeter. There is a dramatically higher parasitic thermal power and very large values of the CIE for the cell without FEC or CO<sub>2</sub>. This cell, as shown in a previous publication, is undergoing surface area increase by Si alloy particle erosion in the base electrolyte.<sup>3</sup>

Figure 4 shows SEM micrographs of a fresh composite Si alloy electrode, and electrodes after they have been cycled for 75 cycles in base electrolyte, base electrolyte with 10 wt% FEC, and base electrolyte saturated with CO<sub>2</sub> (dry ice). The electrode cycled in base electrolyte without any additive (Figure 4b) shows extensive particle

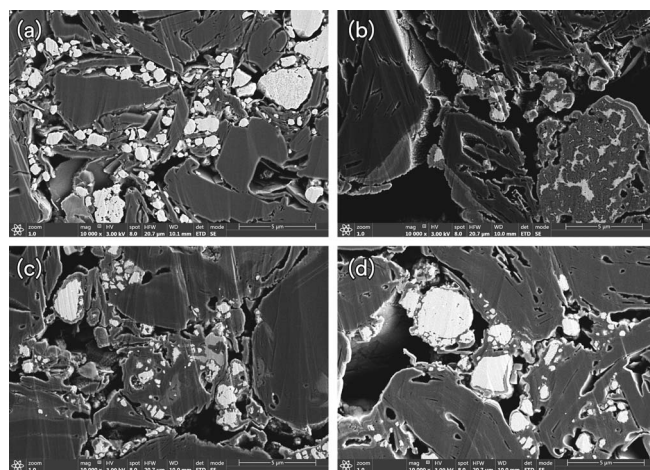


**Figure 4.** FESEM images of cross-sectioned negative electrodes taken from LF129 cells. (a) Fresh, uncycled. (b) Cycled for 75 cycles in base electrolyte (EC/EMC 3/7 1M LiPF<sub>6</sub>), (c) with added 10wt% FEC, and (d) with CO<sub>2</sub> (dry ice). Dark gray corresponds to graphite, light gray corresponds to Si alloy.

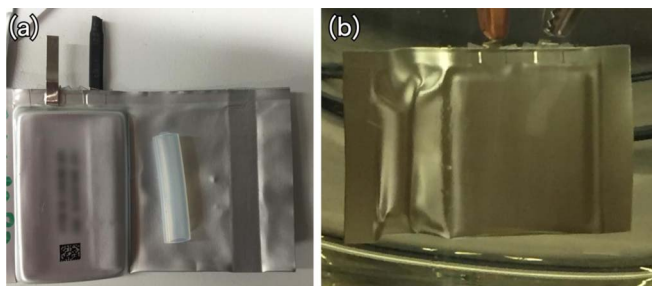


**Figure 5.** (a) Polypropylene tube with pouch cell. (b) Pouch cell submerged in oil for Archimedes measurement with tube sealed inside its pouch extension. Gas produced by the cell has access to the tube.

erosion leading to high surface area of the alloy as measured by isothermal micro-calorimetry.<sup>3</sup> The effect of FEC in the base electrolyte, Figure 4c, shows a significantly different Si particle morphology where little erosion can be seen. Figure 4d shows the cross sectional image of a cell cycled 75 times in the base electrolyte containing CO<sub>2</sub> at an elevated partial pressure. The SEI layer coating the Si alloy particles appears to be substantially thinner than those with 10% FEC. Furthermore, the Si alloy particles cycled in the presence of CO<sub>2</sub> are very similar to uncycled Si alloy particles shown in Figure 4a.

Previous studies have shown that CO<sub>2</sub>, generated by the addition of pyrocarbonates to the electrolyte, will form a passivating SEI interface on graphite.<sup>8,9</sup> Therefore it is not too surprising that such an effect would also occur on Si alloy surfaces. However, the reactivity of CO<sub>2</sub> to Si alloy surfaces during cycling appears to be substantially greater than with graphite. This was determined through the use of the Archimedes principle. The change in volume and buoyancy with CO<sub>2</sub> consumption renders the application of this principle very instructive as shown below.

**Gassing and consumption on formation.**—Figures 5a and 5b show the pouch cells and small polypropylene tubes used to differentiate volume changes due to gas and to electrode dimensional change. Figure 6a shows the voltage curve on formation of two pairs of pouch cells, the LF794 pair has Si alloy while the LF44 does not (further details in Table I). In each pair, one cell had a tube and one cell did not. The tubes had no detectable effect on the electrochemistry of the cells. Figure 6b shows the volume measured for the LF44 cells with and without tubes. A significant amount of gassing (0.5 mL for the cell without the tube) occurred immediately during charge and was partially consumed by the cell for the remainder of the formation cycle. The cell with the tube (dashed line) shows the same overall behavior except that the volume is approximately 0.14 mL less, which corresponds to the tube volume. The results are consistent with the understanding that the initial gas fills the tube and is not detected by the Archimedes method. Based on previous studies, it is expected that the gas produced at low voltage is produced and consumed at the anode during the SEI formation.<sup>14</sup> Figure 6c shows the volume on formation of the LF794 cells, which do contain Si alloy. The cell without the tube (solid line) immediately produced only ~0.1 mL of gas during charge, which is approximately 5x less than the graphite-only cell even though the cells have nearly the same capacity and both have LCO cathodes. In the case of the LF794 cell with the tube, the gas was not sufficient to fill the tube and the volume measurement shows purely the dimensional changes caused by the lithiation and delithiation of the electrodes. Figure 6c is therefore an unambiguous quantification of the gassing and re-absorption of the gas in a cell. Based on past experimental evidence, it is known that CO<sub>2</sub> typically forms the majority of the gas produced during cell formation.<sup>14</sup> Figure 6 suggests that Si alloy leads to significantly increased CO<sub>2</sub> consumption compared to the graphite-only case since these cells both have LCO-based cathodes and artificial graphite-containing anodes. It is this initial result that motivated the present study of the relationship between CO<sub>2</sub> consumption and Si alloy cycling.

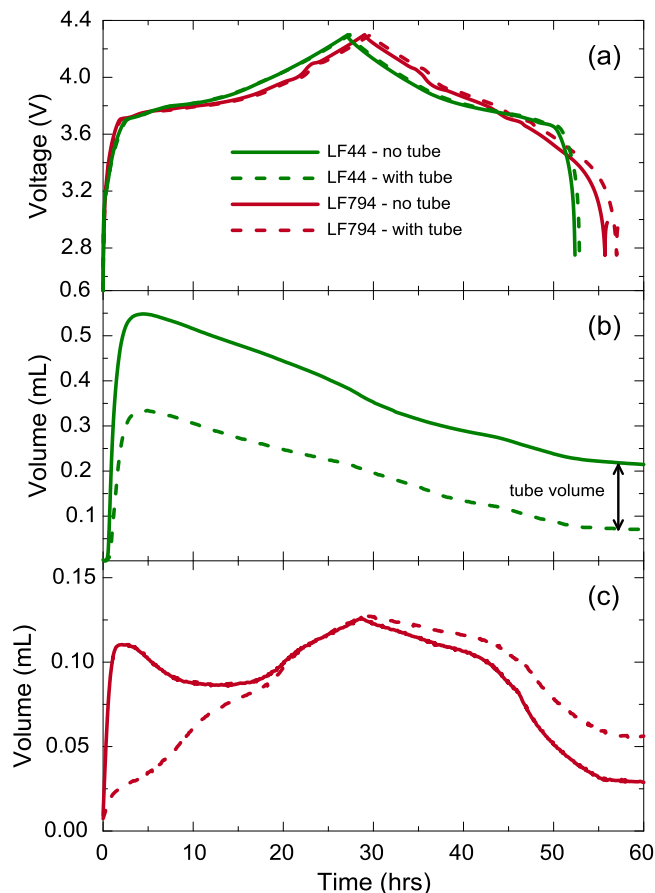


**Figure 6.** (a) Voltage curves of pouch cells during formation. All cells have LCO cathodes. LF44 and LF794 have graphite and graphite/Si alloy anodes, respectively. Dashed lines indicate cells with tubes. (b) Volume of LF44 cells. (c) Volume of LF794 cells.

**CO<sub>2</sub> consumption rate.**—A LF794 cell was filled with base electrolyte and CO<sub>2</sub> added via dry ice as described previously. The cell was then placed in the Archimedes apparatus. Figure 7 shows the voltage and volume of the cell as a function of time. There was no CO<sub>2</sub> consumption during the 24 h 2 V hold and the cell kept its 5.9 mL volume. Consumption began immediately as the cell was charged at 10 mA up to 4.3 V and continued as it was discharged to 2.75 V. The cell then sat at open circuit and CO<sub>2</sub> consumption continued. The

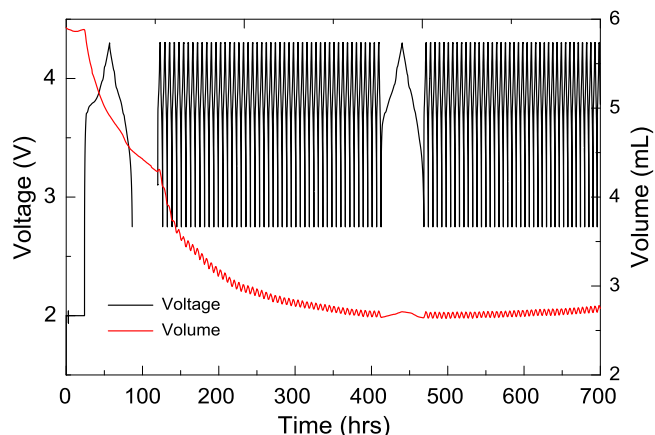


**Figure 7.** Voltage and volume of a LF794 pouch cell containing Si alloy filled with CO<sub>2</sub> (dry ice) during formation and subsequent cycling.

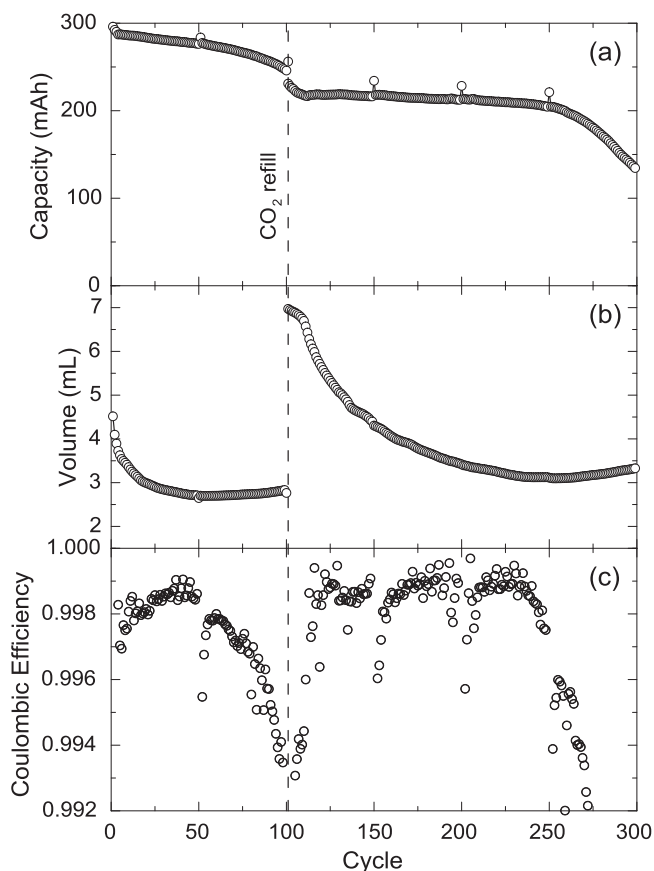


**Figure 8.** (a) Capacity, (b) volume, and (c) coulombic efficiency of a LF794 pouch cell containing Si alloy and CO<sub>2</sub> (dry ice). At cycle 100 the cell was refilled with CO<sub>2</sub> (dry ice).

rate of CO<sub>2</sub> consumption then increased when the cell started being cycled (100 mA up to 4.3 V with a hold to 10 mA, then 100 mA to 2.75 V). The CO<sub>2</sub> consumption continued until slightly after a 10 mA characterization cycle. The minimum in volume (2.6 mL) corresponds to full consumption of the CO<sub>2</sub> and is consistent with the volume of typical cycled cells not containing CO<sub>2</sub>. The oscillation in volume is due to the lithiation and delithiation of the electrodes and is dominated by Si alloy expansion and contraction.

Figures 8a and 8b show the capacity and volume, respectively, as a function of cycle number for the same cell as Figure 7. There is excellent correlation between the increased capacity fade and the exhaustion of the CO<sub>2</sub> as indicated by the minimum in volume. After 100 cycles the cell was taken off the Archimedes apparatus and opened in the dry room, dry ice was then added and the cell was sealed. No liquid electrolyte was added. Cycling and volume measurements were then resumed. The CO<sub>2</sub> refilling is indicated on the plot by the dashed line. Interestingly, for ten cycles following the refill, the capacity continued to decrease and the volume change was minimal. After this apparent “activation period” the capacity retention became excellent and significant CO<sub>2</sub> consumption resumed. At cycle 256 the volume reached its minimum and once again the capacity started falling rapidly and the volume started increasing. Figure 8c shows the CE of the cell. The CE initially peaked at 99.9% and dropped as soon as the CO<sub>2</sub> was completely consumed. Refilling the cell with CO<sub>2</sub> returned the CE of the cell to 99.9%. As the sole additive in the base electrolyte, CO<sub>2</sub> is a strikingly effective additive for Si alloy cycling. Figure 7 and Figure 8 show the clear consumption of CO<sub>2</sub> and dependence of capacity retention on the presence of available CO<sub>2</sub>.

Using the ideal gas law to approximate the CO<sub>2</sub> consumption amounts, one arrives to the conclusion that ~3 mg were consumed during formation, followed by ~3 mg during the next 60 cycles. The

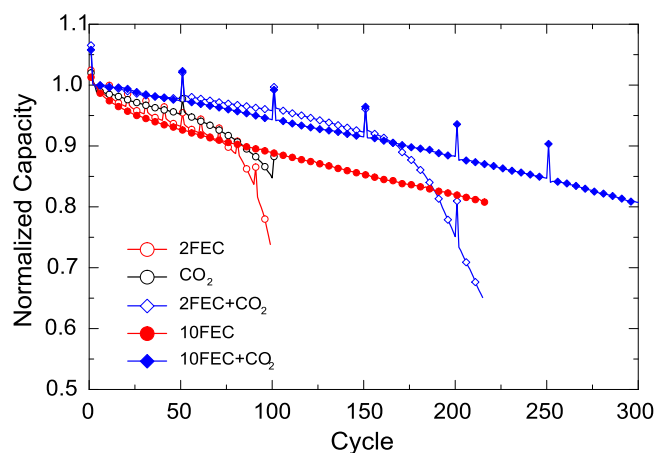


**Figure 9.** Extended cycling of LF794 pouch cells containing Si alloy with base electrolyte and additives as indicate in the legend. CO<sub>2</sub> was introduced via dry ice. Symbols indicate every 5<sup>th</sup> cycle.

cell was then refilled and ~7 mg was consumed over the next 150 cycles. These CO<sub>2</sub> masses are consistent with weight measurements when filling though the error margins are large in both cases and this exercise is simply meant to give an order of magnitude approximation. Nevertheless, this yields a consumption rate during cycling of ~0.05 mg/cycle for a 290 mAh cell. Assuming the CO<sub>2</sub> is primarily consumed by the Si alloy and that the Si alloy makes approximately 45% of the anode capacity this yields a consumption rate of ~0.4 μg<sub>CO<sub>2</sub></sub> · (cycle · mAh<sub>Si</sub>)<sup>-1</sup>. Though this was not investigated in the current study, one would expect a surface area dependence, as well as a time dependence in addition to the cycle dependence as was found in the case of FEC.<sup>2</sup>

**FEC and CO<sub>2</sub>.**—FEC is universally recognized as a key electrolyte component for the cycling of Si-based materials.<sup>1,2,15</sup> An important question to answer is if FEC and CO<sub>2</sub> have additive or synergistic behaviors in Si-containing cells for capacity retention. In order to elucidate this question LF794 cells were prepared to which 2FEC, CO<sub>2</sub>, 2FEC+CO<sub>2</sub>, 10FEC, or 10FEC+CO<sub>2</sub> was added to the base electrolyte. Figure 9 shows the normalized capacity retention of these cells for ease of comparison, though all were close to their designed 290 mAh. All cells were cycled 100 mA up to 4.3 V with hold to 10 mA, then 100 mA to 2.75 V, with the exception of the 10FEC cell which was cycled 30 mA up to 4 V, 20 mA up to 4.25 V then 40 mA down to 3V. Characterization cycles were taken at 10 mA. The 2FEC and CO<sub>2</sub> cells are seen to consume their additive after approximately 60 to 80 cycles, while the 2FEC+CO<sub>2</sub> cell goes through ~160 cycles before sudden failure. Not only do the benefits of FEC and CO<sub>2</sub> appear to be additive, but the capacity retention is improved, suggesting a synergistic effect between CO<sub>2</sub> and FEC. The 2FEC and 10FEC cells initially have identical capacity retention until FEC is consumed in the 2FEC cell.<sup>2</sup> The 10FEC cell continues cycling on track to reach 80% at 250 cycles. The 10FEC+CO<sub>2</sub> cell once again displays improved capacity retention compared to the 10FEC cell and reaches 80% at 300 cycles, once more indicating a synergistic effect between FEC and CO<sub>2</sub>. This of course suggests that while CO<sub>2</sub> still provides a benefit, the addition of FEC to the electrolyte can reduce the amount of CO<sub>2</sub> needed and decreases its consumption rate.

**The use of CO<sub>2</sub> during cell formation.**—Recent papers from the Dahn group have suggested the use of electrolytes containing only a linear carbonate such as EMC as solvent and at least one SEI-forming additive for full cells with high upper cutoff voltages (> 4.3 V).<sup>16,17</sup> In order to verify the SEI forming capability of CO<sub>2</sub>, cells with only EMC in 1M LiPF<sub>6</sub> as the base electrolyte were prepared. The full cells used were LF44 and LF45 cells with graphite-only anodes and

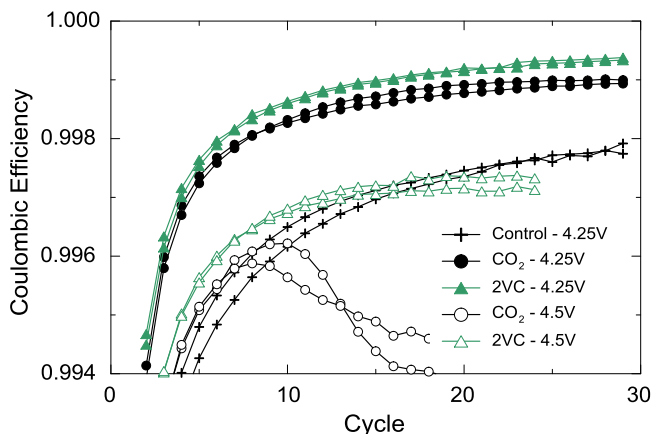


**Figure 10.** Coulombic efficiency of cells cycled in a UHPC at 30°C following a 3 cycle formation and degas. LF44 and LF45 cells (4.25V and 4.5V UCV, respectively, as indicated) contained 1M LiPF<sub>6</sub> in EMC with additives as indicated. CO<sub>2</sub> was introduced via dry ice.

LCO cathodes. In a first series, LF44 cells were prepared with no additives, 2VC, or CO<sub>2</sub>. In a second series, LF45 cells were prepared with 2VC or CO<sub>2</sub>. All CO<sub>2</sub> was added in the form of dry ice. Cycling was performed using an ultra-high precision Novonix cyclor at 20 mA with an upper voltage cutoff of 4.25 for the LF44 cells and 4.5 V for the LF45 cells. Lower cutoff voltages were 3 V for all. All cells underwent 3 cycles at 40°C, were degassed in a dry room, and further cycled at 30°C. Figure 10 shows the coulombic efficiency of all cells. Vinylene carbonate (VC) is known to be an excellent SEI former for graphite. In the 4.25 V series, the cells containing CO<sub>2</sub> have CEs that are much better than control and nearly as good as VC, showing CO<sub>2</sub> is an excellent graphite SEI former and can be used in EC-free electrolytes. It is worth re-iterating that the CO<sub>2</sub> was only present during the 3 initial formation cycles before the cell was degassed. In the 4.5 V series the cells with CO<sub>2</sub> started with similar CEs to the VC cells but quickly fell off. These data show that while CO<sub>2</sub> is very effective at passivating graphite it appears to be unable to play a similar role as VC when cycling to high voltages. These results suggest that VC is able to passivate the cathode surface at high voltage and form an SEI on the graphite while the CO<sub>2</sub> is unable to passivate the cathode at high voltage. Similar experiments, with degassing after formation, were performed with Si-containing cells but showed nearly identical cycling to control cells. This is consistent with the CO<sub>2</sub> consumption results showing the need for continued presence of CO<sub>2</sub> in order to obtain excellent capacity retention in Si alloy cells.

**Room temperature CO<sub>2</sub> electrolyte saturation.**—Previous work has shown FEC is consumed during cycling of Si alloy containing cells and the results above also show consumption of CO<sub>2</sub>. This has important significance for the amount of CO<sub>2</sub> initially charged in the cell. The solubility of CO<sub>2</sub> at room temperature in the base electrolyte of EC/EMC 3/7, 1M in LiPF<sub>6</sub>, is only ~0.4wt%.<sup>18</sup> We also measured the electrolyte parasitic thermal power and cycle life of a cell which had an electrolyte that was prepared by bubbling CO<sub>2</sub> gas through the electrolyte at room temperature. Figure 11 shows the cycle life capacity retention of such a cell compared to a cell that was charged with dry ice. Not surprisingly, the cell with an electrolyte saturated with CO<sub>2</sub> at room temperature shows significant capacity fade. Figures 12a and 12b show comparisons of these two cells in parasitic thermal power and CIE, respectively. Figure 12 indicates the room temperature CO<sub>2</sub> saturated electrolyte was unable to effectively passivate the Si alloy active materials though comparison to Figure 3 shows it was still significantly better than only base electrolyte. This shows that significant amounts of CO<sub>2</sub> are needed to provide optimum passivation, in agreement with the Archimedes results. In all cases the CIE is seen to

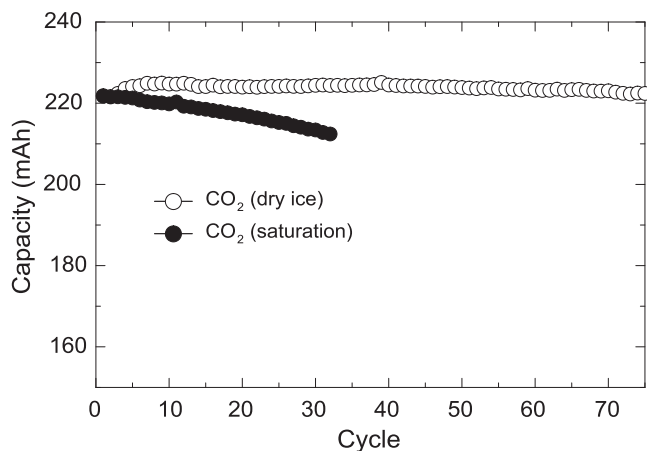


**Figure 11.** LF129 pouch cells containing Si alloy with base electrolyte and CO<sub>2</sub> as indicated in the legend. One cell had CO<sub>2</sub> saturated electrolyte while the other had significantly more CO<sub>2</sub> introduced as dry ice when sealing the cell. See text for details.

correlate with thermal power though the parasitic thermal power is a significantly more sensitive measurement.

## Discussion

To our knowledge the use of CO<sub>2</sub> as an electrolyte component in Li battery chemistry was first noted in metallic Li cells where the presence of CO<sub>2</sub> was found to be beneficial in improving the efficiency and cycle life of rechargeable cells employing a metallic Li electrode. In 1993 and 1994 Aurbach and co-workers published extensive work on the use of CO<sub>2</sub> as an SEI precursor for graphitic negative electrodes in the, at the time, developing field of Li-ion chemistry.<sup>5-7</sup> In 1994 Aurbach, showed that electrolytes that were otherwise extremely poor in producing stable cycling capacity could function quite well when CO<sub>2</sub> was present in the electrolyte. For example, he showed that 1 M LiAsF<sub>6</sub> in gamma-butyrolactone when cycled in a graphite half cell under 6 atm of CO<sub>2</sub> resulted in reversible

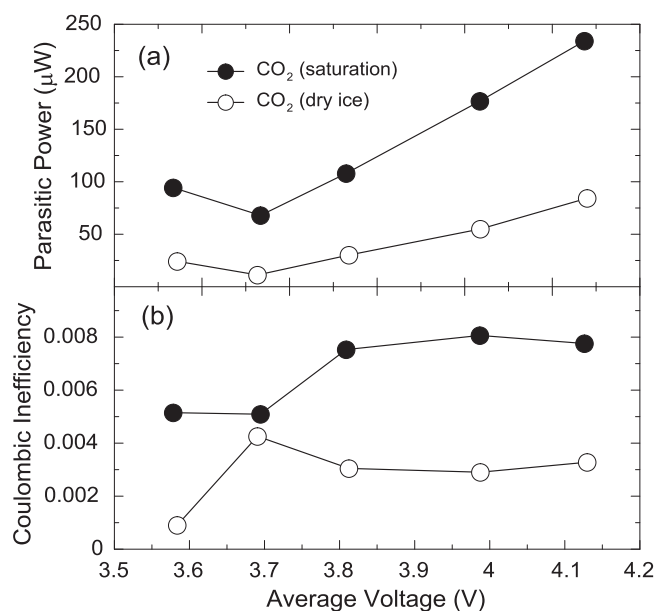


**Figure 12.** (a) Parasitic thermal power, and (b) CIE of LF129 pouch cells containing Si alloy with base electrolyte and CO<sub>2</sub> as indicated in the legend. One cell had CO<sub>2</sub> saturated electrolyte while the other had significantly more CO<sub>2</sub> introduced as dry ice when sealing the cell. See text for details.

graphite intercalation near the theoretical limit while under argon virtually no reversible capacity was found.<sup>6</sup> The surface chemistry of the graphite electrodes in his study were shown to form  $\text{Li}_2\text{CO}_3$  when cycled under a  $\text{CO}_2$  atmosphere. In the same work the authors showed that optimal levels of water contamination also had a dramatic effect on cycle capacity retention. The effect was shown to be due to the hydrolysis of lithium alkyl carbonates to form  $\text{Li}_2\text{CO}_3$ ,  $\text{CO}_2$  and alcohols. In the present work the effect of water is discounted as the injection of additional  $\text{CO}_2$ , shown in Figure 8, results in stabilization of the capacity fade. In the same paper that Aurbach showed the benefit of  $\text{CO}_2$  as an electrolyte additive he also showed that the solvent blend of EC and DEC also produced very good reversible cycling of a graphitic electrode even in the absence of  $\text{CO}_2$ , which is what the vast majority of citing papers have focused on.

An examination of the literature shows that after approximately 1998, little attention at all was paid to  $\text{CO}_2$  as an additive in Li-ion cell electrolyte development and remarkably nothing pertinent to silicon containing electrodes. Solvent blends of EC and linear carbonates and the development of additives, such as VC, seem to have supplanted the need or interest in  $\text{CO}_2$  as an effective SEI precursor for graphitic negative electrodes. However, in 2012 workers at Sanyo reported on the use of  $\text{CO}_2$  as an additive to electrolytes for cells containing sintered negative electrodes containing Si. In this patent an electrolyte blend of EC/DEC 3/7 that was 1M in  $\text{LiPF}_6$  was saturated with  $\text{CO}_2$  at 5°C by bubbling  $\text{CO}_2$  through the electrolyte. They reported a  $\text{CO}_2$  concentration in the electrolyte of 0.37 wt% and a beneficial effect on the cycling of Si.<sup>10</sup> To our knowledge there are no scientific papers on the effect of  $\text{CO}_2$  on silicon and the consumption of  $\text{CO}_2$  by silicon has never been described or quantified.

The present work clearly shows the effect of  $\text{CO}_2$  is greater than that of FEC as an additive in producing stable cycling behavior. The cycling of the LF129 cell shown in Figure 1 is phenomenal for a full cell containing Si, which, apart from being pillowed, has reasonable cell construction, weights, capacities, and electrolyte amount. It is worth noting that while the best LF794 cycling is still obtained with  $\text{CO}_2$ , the LF794 cells do not perform quite as well as the LF129. The root cause is likely that the increased areal capacity leads to mechanical failure in the electrode, which cannot be addressed through electrolyte chemistry. The parasitic thermal power results, Figures 2 and 3, also support the greater effect of  $\text{CO}_2$  and dramatically demonstrate the control of  $\text{CO}_2$  in suppressing the surface area increase of the Si alloy particles (Figures 2–4). Importantly, the elevated  $\text{CO}_2$  amounts used in the present work compared to electrolyte saturated with  $\text{CO}_2$  at room temperature demonstrate the importance of quantities beyond the solubility limit of  $\text{CO}_2$  in conventional electrolytes at atmospheric pressure. While the cell pressures used in this work are certainly well below the 6 atm Aurbach used, they initially exceed atmospheric pressures.

The demonstration of decreased  $\text{CO}_2$  consumption in the presence of FEC and overall improved capacity retention may help understand the role of FEC in improving the capacity retention of Si-based materials. A number of FEC decomposition routes have been proposed and most include LiF and  $\text{CO}_2$  (or  $\text{Li}_2\text{CO}_3$ ).<sup>15,19–21</sup> There have been claims in the literature that LiF is central to FEC's benefit,<sup>15,21</sup> which would suggest F-containing additives as beneficial to Si cycling. On the other hand VC is also seen as beneficial to Si cycling and does not contain any F.<sup>22</sup> In screenings of electrolyte additives, VC was shown to lead to considerable gassing with ongoing cycling<sup>23</sup> and  $\text{CO}_2$  is part of proposed decomposition routes.<sup>20</sup> FEC can also lead to gassing particularly at high temperatures with  $\text{CO}_2$  as the main component.<sup>24</sup> The present results suggest that the possible production of  $\text{CO}_2$  by FEC and VC should be considered when considering mechanisms by which they improve the cycle life of Si-based materials. The primary decomposition product of  $\text{CO}_2$  is likely reduction to  $\text{Li}_2\text{CO}_3$ , as in the case of graphite.<sup>6</sup> Other reaction mechanisms have been proposed where the  $\text{CO}_2$  may react with Li alkoxides (ROLi) to form Li alkyl carbonates (ROCOOLi)<sup>25</sup> or react to form lithium oxalate ( $\text{Li}_2\text{C}_2\text{O}_4$ ),  $\text{Li}_2\text{C}_2\text{O}_3$ , and  $\text{CO}$ .<sup>26</sup> Figure 4 shows unambiguously that the surface reactivity of the Si alloy is mitigated with FEC and even more so with

$\text{CO}_2$ . In both cases it appears the reaction products are dense and insoluble thereby preventing the ongoing reaction of electrolyte with the particle surface. As a  $\text{CO}_2$  reaction product,  $\text{Li}_2\text{CO}_3$  would certainly satisfy these criteria. Beyond these speculations, further studies are certainly needed regarding the chemical composition of SEIs obtained in environments with high partial pressures of  $\text{CO}_2$ .

In screening additives for Li-ion cells having graphite-only anodes, gassing is typically seen as a negative attribute that must be minimized. However, in the case of cells with Si-based materials this may not be true. In over a decade of studying Si-based materials we have never seen an additive that has as strong an impact as  $\text{CO}_2$ . Given the ubiquitousness of  $\text{CO}_2$  and the breadth of activity around Si-based materials, it is surprising that this effect has yet to be recognized in the scientific literature. In our opinion, the results presented here are sufficiently profound as to have the potential to fundamentally change the strategies for additive development and cell design for Si-based materials.

## Conclusions

Carbon dioxide was shown to be an effective additive for extending the cycle life of Li-ion full cells containing a Si alloy and an EC/EMC 3/7 1M  $\text{LiPF}_6$  electrolyte. The graphite/Si alloy negative electrodes contained 15–17 wt% Si alloy having a reversible capacity of 1180 mAh/g, and positive electrodes were  $\text{LiCoO}_2$ . These cells were compared to sister cells with no additives, with FEC, and with a combination of FEC and  $\text{CO}_2$ . Cells were characterized using in-situ isothermal micro-calorimetry, high precision cycling, cross-section imaging and the Archimedes method. In all cases  $\text{CO}_2$  was found to provide a greater benefit compared to FEC, leading to better capacity retention, lower parasitics, thinner SEI, and higher coulombic efficiency.  $\text{CO}_2$  was found to be gradually consumed during cycling and amounts required for ongoing cycling exceed the solubility limit of  $\text{CO}_2$  in conventional electrolytes. Combinations of FEC and  $\text{CO}_2$  were found to provide similar capacity retention benefits as  $\text{CO}_2$ , but with decreased  $\text{CO}_2$  consumption rates.  $\text{CO}_2$  was confirmed to be an effective SEI former on graphite and viable as an additive for EC-free electrolytes in graphite-only cells. Though overlooked by the scientific community as an additive for Si-based materials, this work establishes  $\text{CO}_2$  as a powerful additive leading to an effective SEI layer on Si alloys.

## References

1. M. N. Obrovac and V. L. Chevrier, *Chem. Rev.*, **114**, 11444 (2014).
2. R. Petitbon et al., *J. Electrochem. Soc.*, **163**, A1146 (2016).
3. L. J. Krause, T. Brandt, V. L. Chevrier, and L. D. Jensen, *J. Electrochem. Soc.*, **164**, A2277 (2017).
4. E. Plichta et al., *J. Electrochem. Soc.*, **136**, 1865 (1989).
5. O. Chusid (Youngman), E. Ein-Ely, D. Aurbach, M. Babai, and Y. Carmeli, *J. Power Sources*, **43**, 47 (1993).
6. D. Aurbach et al., *J. Electrochem. Soc.*, **141**, 603 (1994).
7. Y. Ein-Eli et al., *Electrochim. Acta*, **39**, 2559 (1994).
8. F. Coowar, A. M. Christie, P. G. Bruce, and C. A. Vincent, *J. Power Sources*, **75**, 144 (1998).
9. M. D. Levi, E. Markevich, C. Wang, M. Koltypin, and D. Aurbach, *J. Electrochem. Soc.*, **151**, A848 (2004).
10. S. Sawa et al., *USPTO*, US8211569B2 (2012).
11. C. P. Aiken et al., *J. Electrochem. Soc.*, **161**, A1548 (2014).
12. L. J. Krause, L. D. Jensen, and J. R. Dahn, *J. Electrochem. Soc.*, **159**, A937 (2012).
13. L. J. Krause, L. D. Jensen, and V. L. Chevrier, *J. Electrochem. Soc.*, **164**, A1 (2017).
14. C. P. Aiken et al., *J. Electrochem. Soc.*, **162**, A760 (2015).
15. N.-S. Choi et al., *J. Power Sources*, **161**, 1254 (2006).
16. R. Petitbon et al., *J. Electrochem. Soc.*, **163**, A2571 (2016).
17. L. Ma et al., *J. Electrochem. Soc.*, **164**, A5008 (2017).
18. S. Sawa et al., (2012).
19. V. Etacheri et al., *Langmuir*, **28**, 965 (2012).
20. J. M. Martínez de la Hoz and P. B. Balbuena, *Phys. Chem. Chem. Phys.*, **16**, 17091 (2014).
21. H. Nakai, T. Kubota, A. Kita, and A. Kawashima, *J. Electrochem. Soc.*, **158**, A798 (2011).
22. L. Chen, K. Wang, X. Xie, and J. Xie, *Electrochem. Solid-State Lett.*, **9**, A512 (2006).
23. D. Y. Wang et al., *J. Electrochem. Soc.*, **161**, A1818 (2014).
24. V. L. Chevrier et al., *IMLB Conference*, **3**, 299 (2016).
25. S. S. Zhang, *J. Power Sources*, **162**, 1379 (2006).
26. S. E. Sloop, J. B. Kerr, and K. Kinoshita, *J. Power Sources*, **119–121**, 330 (2003).